Experimental Microkinetic Approach of the Photocatalytic Oxidation of Isopropyl Alcohol on TiO_2. Part 1. Surface Elementary Steps Involving Gaseous and Adsorbed C_3H_xO Species

F. Arsac, D. Bianchi,* J. M. Chovelon, C. Ferronato, and J. M. Herrmann

Laboratoire d'Application de la Chimie à l'Environnement (LACE), UMR 5634, Université Claude Bernard, Lyon-1, Bat. Raulin, 43 Bd du 11 Novembre 1918, 69622 Villeurbanne-France

Received: September 20, 2005; In Final Form: January 22, 2006

The present study concerns an experimental microkinetic approach of the photocatalytic oxidation (PCO) of isopropyl alcohol (IPA) into acetone on a pure anatase TiO_2 solid according to a procedure previously developed. Mainly, the kinetic parameters of each surface elementary step of a plausible kinetic model of PCO of IPA are experimentally determined: natures and amounts of the adsorbed species and rate constants (preexponential factor and activation energy). The kinetics parameters are obtained by using experiments in the transient regime with either a FTIR or a mass spectrometer as a detector. The deep oxidation (CO_2 and H_2O formation) of low concentrations of organic pollutants in air is one of the interests of the PCO. For IPA, literature data strongly suggest that acetone is the single route to CO_2 and H_2O and this explains that the present study is dedicated to the elementary steps involving gaseous and adsorbed C_3H_xO species. The microkinetic study shows that strongly adsorbed IPA species (two species denoted nd-IPA_{sads} and d-IPA_{sads} due to non- and dissociative chemisorption of IPA, respectively) are involved in the PCO of IPA. A strong competitive chemisorption between IPA_{sads} and a strongly adsorbed acetone species controls the high selectivity in acetone of the PCO at a high coverage of the surface by IPA_{sads}. The kinetic parameters of the elementary steps determined in the present study are used in part 2 to provide a modeling of macroscopic kinetic data such as the turnover frequency (TOF in s^{-1}) of the PCO using IPA/O_2 gas mixtures.

1. Introduction

In previous works[1−5] and references therein, experimental microkinetic approaches of two catalytic processes have been developed based on the following procedure: (a) a plausible detailed kinetic model of the reaction is adopted, (b) the kinetic parameters of each elementary step are studied experimentally (the coverages of the adsorbed species and either the rate constant: activation energy and preexponential factor, or the adsorption coefficient: heat of adsorption and preexponential factor), and (c) these experimental parameters are used to determine a priori the theoretical catalytic activity (turnover frequency TOF_{th}) of the solid that is compared to the experimental TOF_{ex} values. The experimental data may lead to an adjustment of the elementary steps of the plausible kinetic model.[1,2] This procedure has been applied to the microkinetic studies of (a) the CO/O_2 reaction on Pt/Al_2O_3 catalysts[1,2] and (b) the catalytic oxidation of a diesel soot formed in the presence of a cerium containing additive.[3−5] These studies have shown that the experimental microkinetic approach (denoted EMA) can reveal the elementary steps that control the TOF and as a consequence it can be used as an assisted method of improvement of the catalytic process such as the catalyst development,[5] in line with the perspective imagined by Boudard in the foreword of ref 6 and extended in a more recent article.[7] To develop the EMA of catalytic processes, we have considered the deep (formation of CO_2 and H_2O) photocatalytic oxidation (PCO) in the presence of O_2 (denoted O_2−PCO) of the gaseous isopropyl alcohol (denoted IPA or IPA_g) on TiO_2. The choice of this catalytic system is supported by the following arguments (in addition to the fact that the deep O_2−PCO of organic molecules is a promising process for the removal of diluted VOCs in air): (a) it is well-known that the O_2−PCO of IPA is performed at 300 K on TiO_2 powders[8,9] as well as on single crystals[10−12] that is a favorable situation for experimental microkinetic studies because the low rates of some elementary steps such as the desorption of reactants and intermediates species significantly simplify the calculations linked to TOF_{th}; (b) as compared to previous studies,[1−5] the complex structure of IPA implicates that several successive and/or parallel surface elementary steps such as Langmuir−Hinshelwood steps (denoted L−H step) must be considered to form CO_2 and H_2O; and (c) classical kinetic studies of the PCO of IPA and other organic molecules on TiO_2 have been performed by several authors in the last 30 years[8,9,13−15] providing kinetic data which can be compared with our conclusions.

The global reaction of the deep O_2−PCO of IPA_g is

$$CH_3CHOHCH_3 + 9/2\ O_2 \rightarrow 3\ CO_2 + 4\ H_2O \qquad (1)$$

The first step of the EMA consists adopting a plausible kinetic model. For the CO/O_2 reaction[1,2] and the soot oxidation,[3−5] the number of elementary steps is limited due to the nature of the reactants and products. This explains that there is an agreement in the literature on their detailed mechanisms even if there are discussions of the elementary steps that control the processes. For the O_2−PCO of IPA on TiO_2, there is an agreement to consider that (a) the main gaseous products are acetone, CO_2, and H_2O with a selectivity acetone/CO_2 depending strongly on the experimental conditions[8,9,16,17] and (b) acetone is the main route to the CO_2 formation for the deep oxidation of IPA.[9,15] However, at the difference of the CO and soot oxidations, there

* To whom correspondence should be addressed. E-mail: daniel.bianchi@univ-lyon1.fr.

10.1021/jp055342b CCC: $33.50
Published on Web 03/07/2006

is an open discussion on the detailed mechanism of the O_2−PCO of IPA[8,9,11,16] and this situation imposes a choice of the plausible elementary steps for the development of the experimental procedure.

Plausible Kinetic Model of the PCO of IPA. The discussions on the mechanism of the O_2−PCO of IPA concern the first elementary steps of the transformation of IPA as described below considering two models proposed by Ohko et al.[16] and Brinkley and Engel.[11] There is an agreement in the literature on the elementary steps prior to those involving IPA. The impact of the UV irradiation on TiO_2 is a well-known process[8,16,11] with the formation of electron/hole (e^-/h^+) pairs, according to

$$\text{step } S_a: \quad TiO_2 + h\nu \rightarrow h^+ + e^-$$

It is also accepted that e^- reacts with a molecular adsorbed oxygen species

$$\text{step } S_b: \quad e^- + O_{2ads} \rightarrow {O_{2ads}}^-$$

The mechanisms differ according to the involvement of the hole in the PCO process and the successive elementary steps. Ohko et al.[16] consider that there is a reaction with either an OH group of TiO_2

$$\text{step } S_{c1}: \quad h^+ + OH^-_{ads} \rightarrow {}^\circ OH_{ads}$$

or with an adsorbed H_2O molecule (present in the reactive mixture or produced by PCO)

$$\text{step } S_{c2}: \quad h^+ + H_2O \rightarrow {}^\circ OH_{ads} + {H^+}_{ads}$$

followed by the reaction of the H^+ species with O_2^- (produced in step S_b)

$$\text{step } S_d: \quad {O_2}^-_{ads} + {H^+}_{ads} \rightarrow HO^\circ_{2ads}$$

Ohko et al.[16] consider that the first step of the catalytic transformation of the adsorbed IPA species is the reaction with the °OH radical

$$\text{step } S_e: \quad CH_3{-}CH(OH){-}CH_{3(ads)} + {}^\circ OH_{ads} \rightarrow CH_3C^\circ(OH)\,CH_{3(ads)} + H_2O_{ads}$$

Then $CH_3C^\circ(OH)CH_3$ is involved in different surface elementary steps to form acetone

$$\text{step } S_f: \quad CH_3C^\circ(OH)\,CH_{3(ads)} \rightarrow CH_3COCH_{3(ads)} + {H^+}_{ads} + e^-$$

$$\text{step } S_g: \quad CH_3C^\circ(OH)\,CH_{3(ads)} + O_2 \rightarrow CH_3COO^\circ(OH)\,CH_{3(ads)}$$

$$CH_3COO^\circ(OH)\,CH_{3(ads)} \rightarrow CH_3COCH_{3(ads)} + {H^+}_{ads} + {O_2}^-_{ads}$$

$$\text{step } S_h: \quad CH_3C^\circ(OH)\,CH_{3(ads)} + {HO_2}^\circ_{ads} \rightarrow CH_3COOH(OH)\,CH_{3(ads)}$$

$$CH_3COOH(OH)\,CH_{3(ads)} \rightarrow CH_3COCH_{3(ads)} + H_2O_{2ads}$$

Finally, the different active oxygen containing species react with each other to form stable products. The reaction that dominates this recombination process is considered to be[16]

$$\text{step } S_i: \quad {}^\circ OH + HO_2{}^\circ \rightarrow H_2O + O_2$$

Brinkley and Engel propose a mechanism initiated by a reaction between an adsorbed IPA molecule and a hole[11]

$$\text{step } S_j: \quad h^+ + CH_3CHOHCH_{3(ads)} \rightarrow CH_3(CHOH)^+CH_{3(ads)}$$

The new radical decreases the energy barrier to remove one H^+ via O^{2-} bridging sites of TiO_2

$$\text{step } S_k: \quad CH_3(CHOH)^+CH_{3(ads)} + {O_{bridging}}^{2-} \rightarrow CH_3(CHO)CH_{3(ads)} + {OH_{bridging}}^-$$

The removal of the last hydrogen to produce acetone is performed via OH groups[11]

$$\text{step } S_l: \quad CH_3(CHO)CH_{3(ads)} + {OH_{bridging}}^- \rightarrow CH_3\text{-}CO\text{-}CH_{3(ads)} + H_2O_{(ads)} + \text{vac} + e^-$$

or

$$\text{step } S_m: \quad CH_3(CHO)CH_{3(ads)} + {OH_{Ti}}^- \rightarrow CH_3\text{-}CO\text{-}CH_{3(ads)} + H_2O_{(ads)} + e^-$$

where vac in step S_l and OH_{Ti}^- in step S_m designate a bridging oxygen vacancy and a hydroxyl group coordinated to a Ti site, respectively.[11]

Others initiation steps of the IPA transformation have been proposed such as the reaction with O_2^-.[8] Moreover, Falconer et al.[9,18−20] have shown clearly (in agreement with Bickley et al.[8]) that the PCO of organic species such as IPA, acetic and formic acid can be performed in the absence of O_2 via the U.V activation of lattice oxygen species (denoted $O_{lat.}$) leading to the reduction of TiO_2. The reduced solid can be rapidly reoxidized by O_2 in the dark at 300 K.[19,20] This indicates that others elementary steps must be substituted to step S_b to form an active oxygen species by activation of the oxygen lattice. Whatever the nature of the active oxygen-containing species involved in the reaction, the desorption of acetone and H_2O complete the plausible photocatalytic cycle.

The plausible kinetic model supporting the EMA of the O_2−PCO of IPA can be formulated without considering the totality of the elementary steps proposed by Ohko et al.[16] and Brinkley and Engel[11] due to the fact that the steps with a rate strongly higher that the others do not control the O_2−PCO process and can be omitted. Indeed, it is necessary to know if from adsorbed IPA species (denoted IPA_{ads}) to adsorbed acetone species (denoted Ac_{ads}) (steps S_e−S_h[16] or S_j−S_m[11]) either a single step controls the rate of transformation of IPA_{ads} (rate determining step) or if several elementary steps have similar rates of reaction. In the last case, literature data[21,22] lead to the conclusion that several adsorbed intermediate species must be present with a significant coverage during O_2−PCO of IPA_{ads}. In the first case, only the decrease in the coverage of IPA_{ads} must be observed associated to the possible increase in the coverage of Ac_{ads} (if the rate of consumption of acetone, i.e., desorption and oxidation, is lower than its rate of formation). The evolution of the coverages of the adsorbed species during the O_2−PCO of IPA has been studied by Xu et al.[15] using FTIR spectroscopy. They have shown that, during the initial period of the UV irradiation, all of the IR bands can be ascribed either to IPA_{ads} or to Ac_{ads} (similar results are observed in the present study).

This indicates that the first elementary step of the IPA transformation, either S_e[16] or S_j,[11] is the rate-determining step of the reaction. Note that for a high coverage in acetone other IR bands have been detected by Xu et al.[15] due to different reactions involving Ac_{ads} (i.e: aldocondensation and O_2-PCO of acetone). This allows us to consider in the plausible kinetic model (denoted M1) that only the first elementary step of the IPA_{ads} transformation is kinetically significant. Moreover, there is no clear agreement on the active species involved in this elementary step: either °OH,[16] or h^+,[11] or O_2^-,[8] that is denoted $X^*_{(ads)}$ in the present study. This leads adopting the following series of surface elementary steps for model M1:

S1: adsorption of IPA $IPA_g \rightarrow IPA_{ads}$

S2: desorption of IPA $IPA_{ads} \rightarrow IPA_g$

S3: adsorption of O_2 $O_2 \rightarrow O_{2\ ads} \rightarrow 2\ O_{ads}$

S4: desorption of O_2 $2O_{ads} \rightarrow O_2$

S5: UV formation of the reactive species

$$TiO_2 + h\nu + O_{2ads}\ (\text{or}\ O_{ads}) \rightarrow X_{ads}^*$$

S6: first L-H step $IPA_{ads} + X_{ads}^* \rightarrow I_{1ads} + \Sigma Y_{ads}$

S7: desorption of I_{1ads} $I_{1ads} \rightarrow I_{1g}$

S8: second L-H step $I_{1ads} + X_{ads}^* \rightarrow I_{2ads} + \Sigma Y_{ads}$

The addition of successive elementary steps similar to S7−S8 completes the mechanism for the deep oxidation of IPA (CO_2 and H_2O formation). In steps S6 and S8 (a) ΣY_{ads} represents adsorbed species with a composition and a charge allowing to respect the conservation of atoms and charges and (b) to leave the discussion open we do not identify the I_{1ads} intermediate species; however, literature data[8,9,11,12,15,16] support the view that it is an adsorbed acetone molecule.

Considering that acetone is the main route to CO_2 during deep O_2-PCO of IPA, the EMA has been decomposed into (a) the formation of the acetone intermediate from IPA (present article and part 2) and (b) the oxidation of the acetone into CO_2 (forthcoming article). The present part 1 is dedicated to EMA of the elementary step S1, S2, S6, and S7 considering particularly the competitive chemisorption between reactants and products: Each elementary step is kinetically characterized, in particular considering the impact of the UV light. Part 2 concerns mainly the modeling of macroscopic kinetic data such as the TOF by using the kinetic parameters obtained form the EMA. It is well-known that there is no significant O_2 adsorption at 300 K on a stoichiometric TiO_2 surface: theoretical calculations show that the adsorption of O_2 on a defect-free (perfectly stoichiometric) TiO_2 surface is endothermic while it is exothermic in the presence of oxygen vacancies.[23,24] This last point focuses on the impact of the UV light on the activation of the oxygen species of TiO_2 according to steps S3−S5 and in particular on the role of lattice oxygen species in the process.[9,18−24] At this stage of the study, steps S3−S5 are not detailed into adsorption, dissociation in the dark and with UV irradiation associated to the participation of the oxygen lattice. These elementary steps are studied in detail in part 3, whereas parts 1 and 2 are mainly dedicated to the microkinetic study of the elementary steps involving the gaseous and adsorbed C_3H_xO species (steps S1, S2, S6, S7, and S8). As compared to other studies[8,9,15] that provide a qualitative description of the mechanism of the O_2-PCO, the main contribution of the present EMA is the quantification of the kinetic parameters of the elementary steps of interest and their relations with the TOF taking into account of the nature of the IPA_{ads} and Ac_{ads} species

2. Experimental Section

The TiO_2 catalyst (PC 500 from Millenium, pure anatase) used in the present study has been selected due to its high and stable BET surface area (335 m^2/g after 2 h in helium either at 473 K or at 720 K) which was expected to favor the characterization of adsorbed species by FTIR spectroscopy and experiments in the transient regime with a mass spectrometer as a detector. However, as compared to TiO_2 P25 from Degussa used in numerous studies (BET area $\approx$ 50 m^2/g), the IR transmission at 3800 cm^{-1} is significantly lower for TiO_2 PC 500 (i.e., 1%) than TiO_2 P 25 (i.e., 10%) for the same amount of solid. The role of the impurities in the adsorption properties of TiO_2 is well-known,[25] and those of PC 500 are 0.34 wt % SO_3.

Two analytical systems have been used to characterize (a) the natures and the amounts of the adsorbed species formed by adsorption of IPA and acetone on the TiO_2 surface as well as their evolutions during the O_2-PCO and (b) the kinetic parameters of the elementary steps of model M1. The first analytical system used a FTIR spectrometer (Brucker IFS-28) as a detector with an IR cell (grease free) which was a modified version of that described in more detail previously.[26] Mainly, this homemade IR cell (using Pyrex and Quartz, total volume $V \approx 2$ L) was constituted of three main parts assembled vertically: (a) the top section (Pyrex) was an appropriate system (magnet inserted in Pyrex) to move vertically the quartz sample holder containing the TiO_2 pellet ($\approx$70 mg of TiO_2 powder are compressed to form a disk of diameter $\Phi = 18$ mm), (b) the middle section was a quartz tube ($\Phi = 4$ cm, $L = 35$ cm) fitted out with a furnace associated to thermocouples allowing the pretreatment of the catalyst at high temperatures, and (c) the bottom section (Pyrex) located on the IR beam was mainly constituted by two CaF_2 windows ($\Phi = 35$ mm, thickness $= 3$ mm) positioned on two Pyrex polished flanges (beam path of the IR cell: 8 cm). An appropriate system (Pyrex) allowed repeating the same position of the TiO_2 pellet on the IR beam. Viton O rings (some of them cooled with water jackets) were used to assemble the three parts of the IR cell and to fix the CaF_2 windows to the body of the IR cell. The IR cell was connected by the top section to (a) a classical vacuum production system and (b) a gas introduction system. Between the middle and the bottom section, the UV irradiation of the TiO_2 pellet was performed via an exterior mercury UV lamp: HPK (125 W) from Philips, with a main emission at 365 nm. A water cell was placed in front of the lamp to adsorb near-IR light and to reduce the heating of the TiO_2 pellet. The flux at the position of the pellet was 320 W/m^2 measured with an Oriel radiometer. Before use, the pellet of TiO_2 was treated (removal of organic impurities and dehydration/dehydroxylation) in the quartz section as follows (notation V: vacuum and O: $\approx$ 0.9 atm. of 20% O_2/N_2): V, 300 K→ V, 713 K (10 K/min) → V, 713 K, 2 h → O, 713 K, 2 h → V, 713 K, 10 min→ O, 713 K, 20 min→ O, 300 K→ V, 300 K. The highest temperature, 713 K, prevented the anatase to rutile transformation that occurs near 775 K.[12] The same pellet of TiO_2 was used for several experiments and it was treated as above before each new experiment. After the pretreatment, the sample holder was positioned on the IR beam to study the reversible and irreversible adsorbed species formed by the adsorption of gases in the dark

at 300 K. The partial pressures of IPA, acetone (denoted Ac or Ac_g), and H_2O (denoted P_I, P_A, and P_{H_2O}) were obtained from their vapor pressures at 300 K using individual flasks containing the liquid phases (the liquids were degassed under vacuum before use) and connected to the gas introduction system via different valves. During PCO (pellet in front of the UV lamp), the evolution of the partial pressures P_I, P_A, and P_{CO_2} in the IR cell was followed by FTIR spectroscopy after a calibration procedure using known partial pressures of each gas. The absence of photolysis has been attested by comparing the IPA conversion (C_{IPA} in %) of an IPA/O_2 mixture for the same irradiation duration in the absence ($C_{IPA} = 0\%$) and in the presence ($C_{IPA} = 90\%$) of TiO_2. Moreover, in the presence of TiO_2 and in the absence of UV light there is no significant conversion at 300 K of a IPA/O_2 mixture.

The second analytical system, described in more detail previously,[27] was designed to perform experiments in the transient regime with a mass spectrometer (denoted MS) as a detector. Mainly, various valves allowed us to perform controlled switches between regulated gas flows in the range 100−1000 cm^3/min (at the atmospheric pressure), which passed through the TiO_2 sample contained in a quartz microreactor (volume of ≈2.5 cm^3). The TiO_2 sample ($m = 0.208$ g) was deposited homogeneously on uncompacted quartz wool introduced in the whole volume of the microreactor to favor its homogeneous UV irradiation. A furnace (linear heating rate in the range of 10−300 K/min) was used for the pretreatment of the TiO_2 sample. For the UV irradiation, the furnace was removed, and an UV lamp identical to that used for the FTIR study was positioned in front of the microreactor. The lamp was fitted out on a cylindrical metallic box with polished inside walls to reflect a fraction of the UV light on the microreactor located at the central axe of the box. The gas composition (molar fractions denoted MF or MFs) at the outlet of the reactor was determined using a quadrupole mass spectrometer (with an analysis frequency of 0.66 Hz) after a calibration procedure with gas mixtures of known compositions. The sensitivity and the accuracy on the MF measurements were dependent on (a) the complexity of the gas mixture and (b) the type of transient experiments: the lower detection limit was in the range of 0.2−2 μmol of adsorbed species/g of catalyst and the accuracy was in the range of 2−10%. This analytical system was not well adapted to the quantification of H_2O (interference adsorption processes on the stainless tubes), and this compound was not studied. The temperature of the TiO_2 solid was simultaneously recorded, using a small K type thermocouple (diameter Φ = 0.25 mm) inserted into the quartz wool. This analytical system allowed us to study (i) the adsorption of a gas G (i.e., IPA, Ac, O_2,) at T_a by using a gas flow rate of x% G/y% Ar/He (the MFs of IPA and Ac, i.e., $x = 1.2$ for IPA, were fixed with a saturator/condenser system, Ar was a tracer showing the beginning of the consumption of G), (ii) isothermal and temperature programmed experiments in the transient regime such as desorption in a helium flow and oxidation by using O_2 containing gas mixtures, and (iii) PCO of IPA in the absence and in the presence of O_2 (denoted $O_{lat.}$−PCO and O_2−PCO respectively). Before the adsorption of IPA, the TiO_2 sample was pretreated in gas flows (150 cm^3/min) according to: He, 300 K→ He, 713 K (15 K/min) → He, 713 K, 10 min → 20% O_2/He, 713 K, 0.5 h → 20% O_2/He 300 K→ He.

3. Results and Discussion

According to the EMA, each elementary step of model M1 has been studied as individually as possible using the two analytical systems determining the kinetic parameters of interest.

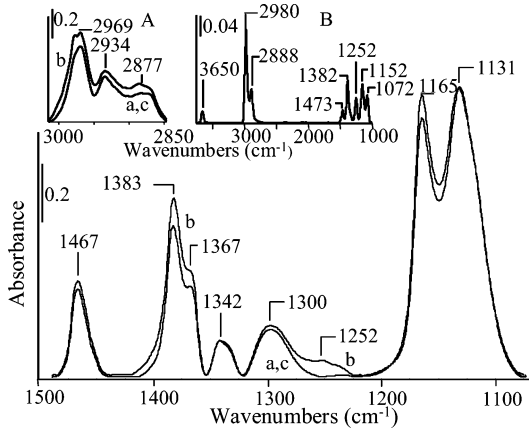

Figure 1. FTIR spectra of the adsorbed IPA species after adsorption of IPA at 300 K (Inset A range 3000−2850 cm^{-1}) on the oxidized TiO_2 solid: (a) in the presence of 131 Pa of IPA, (b) in the presence of 526 Pa of IPA, and (c) after desorption at 300 K. Inset B: FTIR spectrum of the gaseous IPA in the IR cell at 526 Pa.

3.1. FTIR Spectrum of the TiO_2 before Adsorption. The FTIR spectrum of the "as received" TiO_2 sample reveals a large IR band in the range of 3700−3000 cm^{-1} due to hydroxyl groups and an IR band at 1640 cm^{-1} due to un-dissociated H_2O. After pretreatment at 713 K, the FTIR spectrum of TiO_2 at 300 K reveals two overlapped IR bands at 3713 and 3667 cm^{-1} (result not shown) similarly to the observations on TiO_2 P 25:[28,29] 3719 and 3672 cm^{-1}. However, on the present TiO_2 solid, there are in addition two shoulders at 3685 and 3645 cm^{-1}. In line with literature data,[28,29] these four IR bands are ascribed to isolated OH groups formed by the removal of un-dissociated H_2O (T_d < ≈473 K) and the dehydroxylation (T_d >≈ 473 K) of the TiO_2 surface.

3.2. Study of Step S1: Adsorption of IPA in the Dark on Oxidized TiO_2. *Nature of the Adsorbed IPA Species by using FTIR.* The introduction of a small dose of IPA_g (≈10 μmol) on the pretreated TiO_2 solid does not modify strongly the IR bands of the isolated OH groups of TiO_2, whereas a broad IR band is detected in the range of 3500−3000 cm^{-1} due to interacting OH groups associated with new IR bands in the range 3000−2800 cm^{-1} and below 1700 cm^{-1} (result not shown). The increase in P_I leads to the total disappearance of the IR bands of the isolated OH groups and to the strong increase of that of the interacting OH groups indicating either the formation of new OH groups (i.e., dissociation of IPA) or/and the interaction between the adsorbed IPA species and the isolated OH groups. Figure 1 and the insert A gives the IR spectra of the IPA_{ads} species on the oxidized TiO_2 surface after adsorption equilibrium at 300 K for $P_I = 131$ (Figure 1a) and 526 Pa (Figure 1b) (the inset B shows the FTIR spectrum of the gaseous IPA for P_I = 526 Pa). The high intensities of the IR bands after desorption at 300 K (Figure 1c) indicate clearly that IPA forms a large amount of strongly adsorbed species. Moreover, the comparison of Figure 1, panels b and c, indicates that strongly and weakly (removed by desorption at 300 K) adsorbed IPA species (denoted IPA_{sads} and IPA_{wads}, respectively) have very similar IR spectra: only the broad IR band at 1252 cm^{-1} (Figure 1b) that is dependent on P_I (not observed on Figure 1c) characterizes the IPA_{wads} species. The formation of IPA_{sads} and IPA_{wads} species is consistent with the conclusions of Rossi et al.,[29] who observe by using a gravimetric method a two stage process for the adsorption of IPA on TiO_2 (P 25 from Degussa) at 300 K. Moreover, the FTIR spectra in Figure 1c are also consistent with the observation of Rossi et al.,[29] who provide an assignment of the different IR bands (see Table 1 in ref 29). In particular,

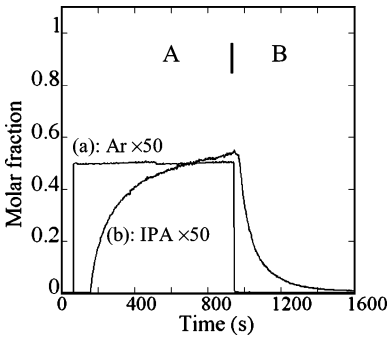

Figure 2. Evolutions of the molar fractions of IPA and Argon in the course of the adsorption and the desorption at 300 K on the oxidized TiO_2 solid. Part A: Adsorption according to He → 1.2% IPA/1% Ar/He. Part B: Desorption in helium.

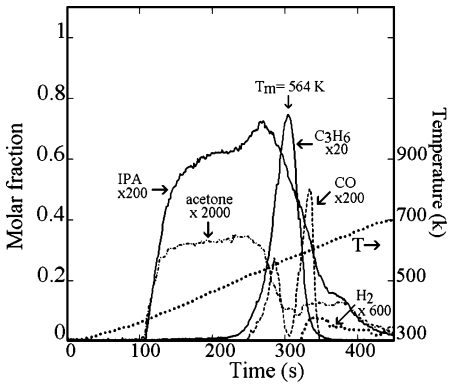

Figure 3. Temperature programmed desorption of the strongly adsorbed IPA species formed at 300 K on the oxidized TiO_2 solid using MS.

the IR band at 1252 cm^{-1} in Figure 1b, corresponds probably to δ_{OH} of a weakly hydrogen-bonded IPA species (denoted H−b-IPA_{wads}), whereas that at 1300 cm^{-1} observed after desorption (Figure 1c) corresponds to the δ_{OH} of a strongly bonded un-dissociated IPA species on $Ti^{+\delta}$ sites (denoted nd-IPA_{sads}).[29] Moreover, the IR band at 1131 cm^{-1} (Figure 1c) can be ascribed[29] to the ν_{C-O} of isopropoxy groups (denoted d-IPA_{sads}) formed by a dissociative adsorption of IPA according to ($CH_3-CHOH-CH_3$ + s + s′→ $CH_3-CHO_{sads}-CH_3$ + s′-H_{ads}, with s and s′ two sites of the TiO_2 surface). It must be noted that similarly to the observations of Rossi et al.[29] an IR band at 1640 cm^{-1} due to undissociated H_2O is detected (not shown in Figure 1) after the formation of d-IPA_{sads} indicating that s′-H_{ads} are probably OH groups that form H_2O at a high coverage. The desorption in a vacuum at 470 K removes the nd-IPA_{sads} species: the IR band at 1300 cm^{-1} is no more detected, whereas that at 1131 cm^{-1} is only slightly decreased indicating that d-IPA_{sads} species are more stable than nd-IPA_{sads}.[29] Finally, after adsorption at 300 K, the two strongly adsorbed IPA_{sads} species can be only differentiated considering the δ_{OH} and ν_{C-O} vibrations. The others vibrations provides IR bands[29] strongly overlapped such as $\nu_{a-CH_3} = 1465-1455$ cm^{-1} and $\nu_{s-CH_3} \approx 1390-1380$ cm^{-1}. In conclusion, we adopt the views of Rossi et al.[29] considering that adsorption of IPA at 300 K on the present TiO_2 solid provides two strongly adsorbed species: nd- and d- IPA_{sads} species (to facilitate the presentation the notation IPA_{sads} is maintained when nd- and d- IPA_{sads} species are not differentiated) and a weakly adsorbed species (H−b-IPA_{wads}). According to the EMA, the role of these three IPA_{ads} species in the PCO of IPA must be considered. Note that the pretreatment of TiO_2 leads to the deep deshydroxylation of TiO_2. However, the formation of d-IPA_{sads} implies that OH groups are formed leading to the rehydroxylation of the surface in agreement with the detection of an IR band of the interacting OH groups similar to that observed on the as received TiO_2 solid (disappearance of the isolated OH groups).

Coverage of the Adsorbed IPA Species at 300 K Using MS Measurements. Figure 2, part A, shows the evolutions of the MFs of the gases at the outlet of the reactor during the adsorption of IPA at 300 K on the oxidized TiO_2 catalyst according to the switch He → 1.2% IPA/1% Ar/He (100 cm^3/min). There is no hydrogen production confirming that d-IPA_{sads} is associated to the formation of OH groups. Figure 2 shows that the MF of IPA is 0 during several seconds of adsorption (comparison with the Ar signal) indicating that IPA_{sads} species are formed according to a nonactivated process (the net adsorption rate is limited by the IPA molar flow rate in the reactor) and then it increases progressively with time on stream indicating the formation of IPA_{wads} species that is consistent with the FTIR observations. In part B of Figure 2, a switch 1.2% IPA/1% Ar/He → He is performed to desorb the IPA_{wads} species. The MF of IPA at the outlet of the reactor before the switch is 1.1 10^{-2} indicating that the adsorption equilibrium of the IPA_{wads} species is not fully attained (it takes several minutes to obtain the inlet molar fraction: 1.2×10^{-2}). The total amount of the IPA consumption in Part A of Figure 2 is given by

$$QIPA_c(300K) = \int_0^{t_a} (\text{curve a} - \text{curve b}) \frac{F}{W} dt \qquad (2)$$

where F is the total molar flow rate, and W is the weight of the sample. Equation 2 provides $QIPA_c(300\ K) = 1255$ μmol/g, that is equal to the total amount of IPA_{sads} and IPA_{wads} species: $QIPA_{sads}$ and $QIPA_{wads}$, respectively. An expression similar to (2) provides $QIPA_{wads}$ from the data in part B of Figure 2: $QIPA_{wads} = 307$ μmol/g leading to $QIPA_{sads} = 948$ μmol/g or 2.82 μmol/m^2 of solid. This last value is consistent with literature data on different TiO_2 solids: 3[29] and 2.7 μmol/m^2,[8] whereas a higher value is determined by Larson et al.:[9] 6.9 μmol/m^2. Strongly higher values such as 4.4×10^{16} molecules/cm^2 (731 μmol/m^2) using a 1000 ppmv IPA_g containing gas mixture[16] indicate that IPA_{wads} species are involved in the measurements. Assuming a total number of superficial sites of $\approx 10^{15}$ sites/cm^2, it comes that the amount of IPA_{sads} at 300 K on the present TiO_2 solid corresponds to 16% of the sites of TiO_2. Those adsorption sites of IPA are denoted s_1 and they must be constituted by either $Ti^{+\delta}$ or couple of $Ti^{+\delta}$ according to the literature data.[29] There is a large number of free sites for (a) the adsorption (or readsorption) of intermediates species of the O_2-PCO of IPA and (b) the activation of O_2. Note that nd- and d-IPA_{sads} cannot be quantified separately by the present analytical procedure.

3.3. Study of Step S2: Desorption in the Dark of the IPA_{ads} Species. *Temperature Programmed Desorption using MS.* Figure 3 gives the TPD spectrum observed after the experiments in Figure 2. There is no desorption before 375 K indicating that the IPA_{wads} species is totally desorbed after a long helium purge at 300 K. For $T_a > 375$ K, IPA desorbs according to two overlapped broad TPD peaks with maximum at $T_M = 437$ K and $T_M = 512$ K respectively (total amount, 232 μmol/g). In parallel to the desorption of IPA, a very small acetone production is detected (at the limit of the detection of the experimental procedure): ≈ 5 μmol/g. At $T_d > 457$ K, a strong production of propylene is observed with a maximum at 564 K: 720 μmol/g associated to two CO peaks at 542 and 597 K (this last peak is associated with traces of hydrogen):

total amount 54 μmol of CO/g. Traces of CO_2 (not shown) are observed at $T_d > 550$ K: 13 μmol/g. At the end of the TPD, a switch He $\rightarrow$ 10% O_2/3%Ar/He is performed (not shown) to oxidize the remaining adsorbed carbonaceous species according to an isothermal oxidation leading to the production of CO_2: 25 μmol/g. The C mass balance during TPD and oxidation at 713 K, 2978 μmol of C/g is consistent with the amount of $IPA_{sads} = 948 \times 3 = 2844$ μmol of C/g, considering the accuracy of the experimental procedure. Adsorption of propylene at 300 K on the oxidized TiO_2 has been studied similarly to IPA by using 1% C_3H_6/2% Ar/He followed by a TPD procedure (results not shown). A single small C_3H_6-TPD peak, 64 μmol/g, is observed at 364 K without production of CO_2 during oxidation at 713 K. This indicates that the propylene peak in Figure 3 is not linked to the desorption of a strongly adsorbed propylene species formed at lower temperatures during the TPD process: it is due to the fact that, for $T_d > 500$ K, an IPA_{sads} species evolves according to two processes: (a) it desorbs as IPA_g and (b) it is transformed to propylene by a surface reaction such as $CH_3-CHO_{ads}-CH_3$ (d-IPA_{sads} species) $\rightarrow$ $(CH_3-CH=CH_2)_g + OH_{ads}$ (the OH_{ads} groups may produce H_2O at high temperatures). The results in Figure 3 are consistent with literature data for the TPD of IPA_{sads} species on TiO_2 P25 from Degussa[9] and TiO_2 anatase from American Instrument Co (10.3 m^2/g);[30] that is, IPA starts to desorb at 325 K according to two overlapped broad peaks while the propylene peak is observed at 550 K.[9] There are minor differences between Figure 3 and the observations of Larson et al.[9] on the acetone and CO productions that are probably linked to slight differences in the surface of the two solids as revealed by the IR bands of the OH groups. Note that Rekoske and Barteau[31] have studied particularly the kinetic and the selectivity of the thermal IPA conversion on TiO_2 in the temperature range of 448−598 K in the presence and in the absence of O_2, showing that propylene as well as acetone can be formed with a higher selectivity in acetone at low temperatures (IPA conversion <4%). This is consistent with the small production of acetone during the TPD at 375 K < T_d < 457 K. Note that the amounts of IPA and propylene detected during the TPD in Figure 3 do not necessary quantify the amounts of nd- and d-IPA_{sads} species respectively formed at 300 K because it is not excluded that a significant fraction of nd-IPA_{sads} dissociates during the TPD process to produce d-IPA_{sads}.

The broad IPA-TPD peak in Figure 3 reveals clearly that there is an increase in the activation energy of desorption (denoted E_{dI}) of the IPA_{sads} species according to their coverage (denoted θ_I) on the TiO_2 surface. However, the determination of E_{dI} as a function of θ_I, using the data in Figure 3, is not accurate because the design of the present experiment is significantly different than that deduced from literature criteria to validate the TPD measurements.[32−34] The curve $E_{dI} = f(\theta_I)$ has been obtained using the evolution of the IR bands of IPA_{sads} during isothermal desorption.

Determination $E_d = f(\theta_I)$ using FTIR Spectroscopy. After the adsorption of IPA at 300 K, the IPA_{wads} species is removed by desorption in a vacuum. Then the TiO_2 pellet is heated at increasing temperature ($\Delta T = 50$ K) for a duration $t_d = 15$ min before it is to be positioned on the IR beam. The progressive decrease in the IR bands of IPA_{sads} is observed for $T_d > \approx 400$ K without the appearance of new IR bands. This confirms that the two IPA_{sads} species neither desorb at $T_d < 400$ K nor are transformed to new strongly adsorbed species that is a result consistent with Figure 3. The E_{dI} values as a function of θ_I have been determined studying the evolution of the intensity of the IR band at 1467 cm^{-1} (due to nd- and d-IPA species) with the duration t_d of the desorption at 423 K. Curve ○ in Figure 4 shows the evolution of θ_I with t_d: θ_I = (IR band area at t_d)/(IR band area at $t_d = 0$). The decrease in θ_I can be followed by FTIR even for a very low rate of desorption preventing the impact of diffusion processes to the measurements.[34] The activation energies of desorption are determined by the comparison of the experimental curve with the theoretical curve obtained solving numerically

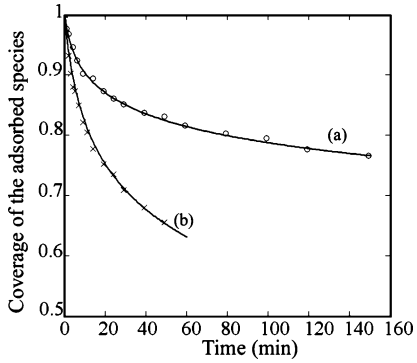

Figure 4. Determination of the activation energy of desorption of IPA_{sads} and Ac_{sads}: (○) experimental (IR band at 1467 cm^{-1}) and (a) theoretical evolutions of the coverage the IPA_{sads} species during isothermal desorption at 423 K, respectively; (×) experimental (IR band at 1696 cm^{-1}) and (b) theoretical evolution of the coverage of the Ac_{sads} species during isothermal desorption at 323 K (see the text for more details).

$$\frac{-d\theta_I}{dt} = k_{dI}\theta_I \qquad (3)$$

with k_{dI} the rate constant of desorption and considering that E_{dI} is a function of θ_I: $k_{dI} = \nu \exp(-E_{dI}(\theta_I)/RT)$. Curve a in Figure 4 is obtained assuming in expression (3) that (a) the preexponential factor of k_{dI} is $\nu = (kT/h)$ according to the statistical thermodynamics,[35] with k and h the Boltzmann's and Planck's constants respectively and (b) that E_{dI} increases linearly with the decrease in θ_I: $E_{dI}(\theta_I) = [E_{dI}(1) + (1 - \theta_I)(E_{dI}(0) - E_{dI}(1))]$ with $E_{dI}(0)$ and $E_{dI}(1)$ the activation energies of desorption at $\theta_I = 0$ and 1, respectively. Curve a that overlaps the experimental data is obtained considering that $E_{dI}(1) = 118$ and $E_{dI}(0) = 178$ kJ/mol. The experimental data in Figure 4 are obtained at a temperature where mainly desorption of IPA_g is detected in Figure 3. This indicates that the decrease in θ_I from 1 to 0.75 in Figure 4 corresponds mainly to the nd-IPA_{sads} species that is consistent with the fact that the IR band at 1131 cm^{-1} is only slightly decreased during the isothermal desorption. This means that the fraction of IPA_{sads} producing propylene during TPD (Figure 3) may have E_{dI} values higher than 178 kJ/mol. The strong dependence of E_{dI} on θ_I indicates the heterogeneity of the s1 sites corresponding to $Ti^{+\delta}$ sites in different environments. The E_{dI} values (equal to the heat of adsorption considering non activated chemisorption) are consistent with the microcalorimetric measurement of Rossi et al.,[29] who indicate a variation of the heat of adsorption of the IPA_{sads} species with the coverage from 145 to 220 kJ/mol according to a roughly linear profile. Moreover, they determine that more weakly bonded IPA species have a heat of adsorption in the range 50−145 kJ/mol. For the 100−145 kJ/mol range, the notion of weakly/strongly adsorbed species based on a isothermal desorption is dependent on the exact temperature and on the duration of the desorption. For the EMA of the PCO of IPA, the present E_{dI} values show that at 300 K, the elementary step

S2 cannot contribute significantly to the rate of disappearance of IPA_{sads} species. This conclusion is important because it must be considered (as assumed in the present study) that if the IPA_{sads} species are the adsorbed intermediate of the PCO (and not IPA_{wads} species) then step S6 can be studied independently of step S1 (without IPA_g). This is a favorable situation for the EMA because the theoretical rate of an adsorption step[35] is very high (see below) and as discussed previously[36] for the microkinetic study of the CO/O_2 reaction, the experimental rate of adsorption is controlled by diffusion processes that are difficult to be characterized by experimental procedures.

3.4. Study of Step S6 in the Dark. The introduction of O_2 at 300 K after the formation of IPA_{sads} neither modifies the IR spectrum of the adsorbed species nor leads to the production of new gaseous compounds (MS): the IPA_{sads} species are not modified in the absence of UV irradiation. These observations are consistent with the results of Barteau et al.,[30,31] who observe the thermal dehydration and the deep oxidation of IPA on TiO_2 only for $T > 448$ K.

3.5. Study of Step S6 with UV Irradiation. Several kinetic parameters must be determined to characterize step S6 such as the dependence of the rate on P_{O_2} and P_{H_2O} (formed during the PCO), the rate constant k_6, and the nature of I_{1ads}. Literature data strongly support the view that I_{1ads} is an adsorbed acetone molecule, indicating that there are (a) no other significant coverage of the intermediates species involved in the detailed mechanisms[11,16] and (b) no significant others routes to CO_2 than Ac_{ads}. These different points have been studied on the present TiO_2 solid.

Acetone as Single Significant Route of the Deep PCO of IPA. To confirm that acetone is the main route to CO_2, we have performed an O_{lat}-PCO of IPA_{sads} (in the absence of O_2) in line with the studies of Falconer et al.,[9,18−20] to limit the conversion of I_{1ads} according to step S8. Using the MS system, after adsorption of IPA at 300 K on TiO_2 followed by the desorption of IPA_{wads} (Figure 2), the solid is UV irradiated in a helium flow (result not shown). It is observed (a) the absence of IPA desorption and (b) the formation of gaseous acetone when the UV lamp is turned on (without detectable CO_2) with a rate decreasing progressively with time on stream according to a profile similar to that observed by Larson et al.[9] on TiO_2 P 25. The average rate of acetone production (denoted R_{Acg}) during the first 15 min of O_{lat}-PCO is 0.23 μmol/(g·min), whereas Larson et al.[9] determine ≈ 1.2 μmol/(g·min) in the presence of 30 ppm of O_2. Moreover, the color of the TiO_2 sample changes from white to gray blue and then to dark blue for long irradiation duration indicating the progressive reduction of the TiO_2 sample.[37,38] These observations show that there is no significant CO_2 production in experimental conditions preventing the PCO of acetone. This supports the view that there are no other routes with a significant rate for the deep O_2−PCO of IPA_{sads} than the formation of acetone. This conclusion is confirmed by new experiments in Part II of the present study.

Characterization of the Acetone Adsorbed Species. The literature data strongly suggest that the intermediate species of the O_2−PCO of IPA is an adsorbed acetone molecule. To confirm this view on the present TiO_2 solid, we have studied by using FTIR spectroscopy (Figure 5), the strongly adsorbed acetone species (denoted Ac_{sads}) formed by the adsorption of Ac_g at 300 K on a clean TiO_2 surface followed by a vacuum purge of the IR cell. In the presence of Ac_g, the spectrum is identical to that in Figure 5, the vacuum purge only leads to a decrease in the intensity of the IR bands by 35%. The spectrum

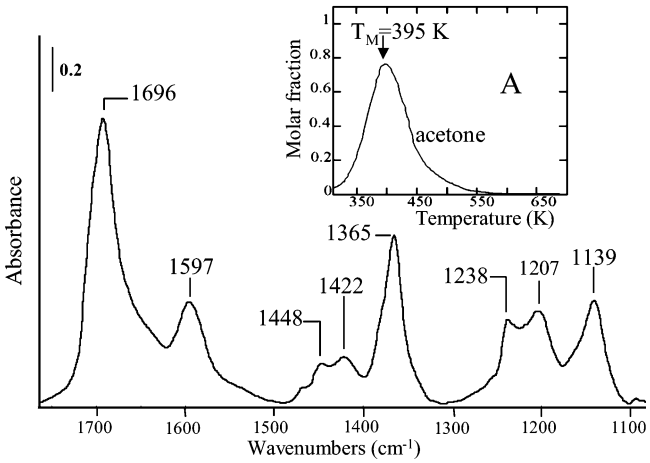

Figure 5. FTIR spectrum of the strongly adsorbed species formed by adsorption of acetone at 300 K on the oxidized TiO_2 solid after 15 min of adsorption. Inset A: TPD spectrum of the strongly adsorbed acetone species formed at 300 K using MS.

in Figure 5 is in line with literature data, and there is an agreement to assign the main IR bands to a non dissociative Ac_{sads} species formed on the Lewis sites of TiO_2 (i.e., $(CH_3)_2$−CO−$Ti^{+}\delta$): 2971 and 2939 cm^{-1} (not shown, ν_{C-H}), 1696 cm^{-1} (highest IR band, $\nu_{C=O}$), 1422 cm^{-1} (δ_{asCH3}), 1365 cm^{-1} (δ_{sCH3}), and 1238 cm^{-1} (ν_{C-C}).[15,28,39,40] The exact positions of the IR bands depend on the Lewis sites.[39] It is well-known that Ac_{sads} is slowly transformed in the dark at 300 K to form different strongly adsorbed species such as adsorbed mesityl oxide (MSO) and diacetone alcohol (DAA) leading to new IR bands with intensities depending on the rates of the surface reactions.[39,40] Several minor IR bands in Figure 5 can be ascribed either to these compounds or to adsorbed intermediates species of this aldol-condensation type of reaction.[28,39] For instance, the IR bands at 1597 and 1448 cm^{-1} that increase progressively with the duration of the adsorption are due to ν(C═C) and $\delta_{as}(CH_3)$, respectively, of MSO.[28] However, during O_2−PCO of Ac_{ads} (results to be published), the IR bands due to MSO remain very low indicating that the surface reactions in the dark involving the Ac_{sads} species do not participate significantly in the observations during PCO. This is probably linked to the observations of Luo and Falconer,[41] who have shown that the rate of the aldol condensation of acetone is significantly lower on a pure anatase TiO_2 than a mixture of anatase and rutile. The comparison of the IR spectra of the IPA_{sads} (Figure 1) and of Ac_{sads} (Figure 5) shows that there is an overlap of the IR bands in several regions excepted for the IR bands at 1696 and 1467 cm^{-1} that characterize Ac_{sads} and IPA_{sads}, respectively. This situation allows us (a) to identify clearly the presence of Ac_{sads} during the PCO of IPA_{sads} and (b) to follow how the IPA_{sads} species are converted to Ac_{sads} during PCO of IPA in line with literature data.[15, 28]

Identification of the I_{1ads} Species. After adsorption of IPA at 300 K, followed by a desorption in a vacuum to remove IPA_{wads}, $P_{O_2} = 1.9 \times 10^4$ Pa is introduced using a 20% O_2/N_2 mixture. The evolutions of the adsorbed species during O_2−PCO are determined by repeating the following cycle: (a) the UV lamp is turned on for 15 min to stabilize the emission; (b) the TiO_2 pellet is positioned in front of the lamp for an irradiation duration t_i and then it is positioned on the IR beam to study the modification of the adsorbed species. After each irradiation duration, the composition of the gas phase in the IR cell is determined by FTIR. Figure 6, part A, shows the evolutions of the FTIR spectra with the total irradiation duration: $TI = \Sigma t_i$.

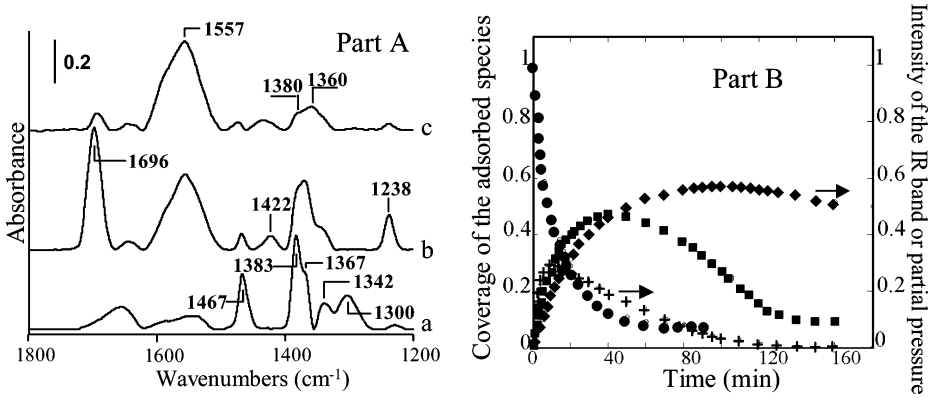

Figure 6. FTIR study of the static O_2-PCO (P_{O_2} = 1.9 10^4 Pa) of the IPA_{sads} species. Part A: Evolution of the FTIR spectra of the adsorbed species with the duration TI of the O_2-PCO; (a−c) TI = 0, 30, 120 min. Part B: (● and ■) coverages of the IPA_{sads} and Ac_{sads} species, respectively; (+) partial pressure (Torr) of acetone; (◆) intensity of the IR band at 1557 cm^{-1} (formate species).

It can be observed that the IR bands of IPA_{sads} (i.e., 1467 cm^{-1}) (spectrum a) decrease progressively with the increase in TI (spectrum b), whereas in parallel, new IR bands, similar to those observed in Figure 5 for Ac_{sads} (in particular that at 1696 cm^{-1}), increase during the first 40 min and then decrease progressively (spectrum c). The IR band at 1640 cm^{-1} is due to undissociated H_2O formed in part during the adsorption of d-IPA_{sdas}.[29] A broad IR band at 1557 cm^{-1} (spectra b and c), probably due to the overlap of two IR bands (a shoulder is observed at ≈ 1565 cm^{-1}) associated with strongly overlapped IR bands of lower intensity in the range 1385−1350 cm^{-1} increases with TI and then dominate the IR spectra for TI > 120 min (the IR band at 1696 cm^{-1} is very weak in spectrum c). A strong IR band at 1557 cm^{-1} can be ascribed to the asymmetric stretching of COO groups present in adsorbed species such as formate and carbonate species (uni- and bidentate carbonate and carboxylate),[42] whereas the IR band of the symmetric stretching of these groups is situated in the range 1420−1350 cm^{-1}.[42] In addition, adsorbed formate species give an IR band at ≈1380 cm^{-1} due to the C−H (bending in the plan).[42] Similar IR bands are present in spectrum c of Figure 6; however, the strong overlap of the IR bands does not allow a clear identification. For a long duration of the O_2-PCO of acetone on TiO_2, El-Maazani et al.[28] observe IR spectra similar to spectrum c Figure 6A, that they ascribed to a bidentate formate, whereas during the O_2-PCO of IPA_{sads}, Xu et al.[15] observe the increase of an IR band at 1560 cm^{-1} that they ascribe also to a formate species. Finally, the assignment of the intense IR at 1557 cm^{-1} to formate species is favored.[15,28,42] Note that the increase in the IR band at 1557 cm^{-1} in parallel to that of the Ac_{sads} species at 1696 cm^{-1} (spectrum b) may suggest that it is linked to an intermediate species of the detailed mechanism proposed by Ohko et al.[16] for the IPA transformation into acetone. However, for large TI values, the comparison of spectra b and c shows clearly that the IR band (1696 cm^{-1}) due to the final product decreases, whereas that at 1557 cm^{-1} remains unchanged proving that the adsorbed species characterized by the IR band at 1557 cm^{-1} is formed by the transformation of the Ac_{sads} species. This confirms that the coverages of the intermediates species of the transformation of IPA_{sads} to Ac_{sads} are very small and undetectable justifying the formalism of step S6 of the kinetic model M1.

Evolution on the Coverage of TiO_2 during O_2-PCO of IPA_{sads} using FTIR. Curves ● and ■ in Figure 6B show the evolutions with TI of θ_I and θ_A the coverage of Ac_{sads} species, respectively. The θ_I values are obtained using the ratio [A(1467 cm^{-1}) at TI]/[A(1467 cm^{-1}) at TI= 0] where A(1467 cm^{-1}) is the absorbance of the IR band at 1467 cm^{-1} (Figure 6A). The θ_A values are obtained using the ratio [A(1696 cm^{-1}) at TI]/[A(1696 cm^{-1}) measured after adsorption of Ac_g on a clean TiO_2 surface (Figure 5)]). It can be observed that (a) θ_I decreases progressively indicating its transformation according to step S6 and (b) θ_A increases and then decreases with a maximum at TI = 40 min that is the situation expected for an adsorbed intermediate species in successive reactions.[21,22] Curve ◆ in Figure 6B provides the evolution of the intensity of the IR band at 1557 cm^{-1}: it indicates an accumulation of the "formate" species during the PCO followed by a very slow decrease. Curve + in Figure 6B, provides the evolution of the partial pressure P_A of Ac_g, in the IR cell during the static O_2-PCO of IPA_{sads}. This curve indicates that a significant fraction of acetone desorbs during the first minutes of the reaction (at high coverage of IPA_{sads}) before its consumption. Note that the maximum in P_A is at a TI value lower than that of θ_A. This is clearly unexpected considering the plausible kinetic model M1 because the formation of Ac_{sads} (step S6) and of P_A (step S7) are successive. This means that some elementary steps of model M1 must be modified considering these experimental observations. One of the intent of the present microkinetic study (present article and part II) is to provide a kinetic modeling of the experimental data in Figure 6B by using a modified version of the kinetic model M1 as described in Part II.

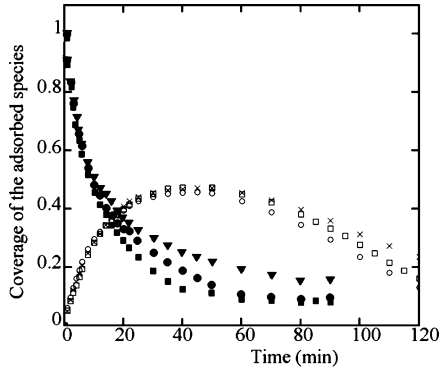

Figure 7. Impacts of the experimental conditions on the evolution of the coverages θ_I of IPA_{sads} and θ_A of Ac_{sads} with the duration TI of the O_2-PCO of IPA_{sads}. (● and ○) θ_I and θ_A with P_{O_2} = 19 kPa; (▼ and ×) θ_I and θ_A with P_{O_2} = 1.9 kPa; (■ and □) θ_I and θ_A with P_{H_2O} = 790 Pa and P_{O_2} = 19 kPa.

Impacts of the Experimental Conditions on the O_2-PCO of IPA_{sads}. These impacts are revealed by the modification of the rate of disappearance of IPA_{sads} species. For instance, curves ● and ▼ in Figure 7 give the evolution of θ_I during O_2-PCO using P_{O_2} = 19 and 1.9 kPa, respectively. The overlap of

the two curves shows that $P_{O_2} > 1.9$ kPa has no impact on the rate of disappearance of IPA_{sads}. Similarly, curve ■ is obtained in the presence of $P_{H_2O} = 790$ Pa, introduced after the formation of IPA_{sads} and before the introduction of $P_{O_2} = 19$ kPa. The comparison of curve ■ with curve ● shows that H_2O has no significant impact on the rate of conversion of IPA_{sads}. The experimental data in Figure 7 show clearly that the active species X^*_{ads} in step S6 of the model M1 is dependent significantly neither on P_{O_2} ($P_{O_2} > 1.9$ kPa) nor on P_{H_2O}. Considering the mechanism of Ohko et al.[16] the absence of impact of P_{H_2O} must be due to the fact that at high θ_I values (as used in the present study), the formation of d-IPA_{sads} provides a large amount of OH groups, limiting the impact of P_{H_2O}.

3.6. Study of Step S7 and Modification of the M1 Model. The difference in the maximums of θ_A and P_{Ag} in Figure 6B leads to the conclusion that the kinetic model M1 must be modified. As described below this is due to the competitive chemisorption between IPA_{sads} and Ac_{sads} (in line with an early study)[8] imposing to reconsider step S7.

Comparison of the Amounts of IPA_{sads} and Ac_{sads} Species. Using the MS system, a TPD is performed after adsorption of acetone at 300 K followed by the desorption in helium of the weakly adsorbed species. The inset A in Figure 5 shows that a single sharp acetone TPD peak is observed, 330 μmol/g, at $T_m = 395$ K that is a value consistent with the observations of Larson et al.[9] on TiO_2 P 25: $T_m = 425$ K. After the TPD, the introduction of O_2 at 713 K leads to the formation of CO_2 (not shown): 222 μmol of CO_2/g. This amount is probably linked to the formation, during the TPD, of strongly adsorbed mesityl oxide (MSO) and diacetone alcohol (DAA).[39,40] The amount of Ac_{sads} species at 300 K is $(330 + 222/3) \approx 404$ μmol of acetone/g (1.2 μmol/m^2) that is a value significantly lower than that of the IPA_{sads} species: 948 μmol of IPA/g. On TiO_2 P 25, Larson et al.[9] determine a higher amount of adsorbed acetone species, 4.9 μmol/m^2, in agreement with the fact that they have observed an higher amount of IPA_{sads}. Xu et al.[15] determine 8.3 μmol/m^2 at 300 K after the adsorption equilibrium (titration of weakly and strongly adsorbed species). The amount of Ac_{sads} (404 μmol/g) indicates that a competitive chemisorption between IPA and acetone may concern roughly 42% of the s_1 sites adsorbing IPA_{sads}. To quantify the competitive chemisorption between IPA and acetone, the activation energy of desorption of acetone has been determined according to the procedure used for the IPA_{sads} species.

Activation Energy of Desorption of Ac_{sads} and Expected Competitive Chemisorption. After the adsorption of acetone, the evolution of the intensity of the IR band at 1696 cm^{-1} is studied during an isothermal desorption at 323 K. This provides the evolution of the coverage of Ac_{sads} (Figure 4 curve ×) by using the area of IR band at 1696 cm^{-1}: $\theta_{Ac.}$ = (IR band area at t_d)/(IR band area at $t_d = 0$ s). Curve b in Figure 4 that overlaps the experimental data is obtained using an expression similar to (3) with $E_{dAc}(1) = 87$ to $E_{dac}(0) = 108$ kJ/mol. These values are lower than those of the IPA_{sads} species indicating that if IPA_{sads} and Ac_{sads} are adsorbed on the same sites (competitive chemisorption) then IPA_{sads} must displace Ac_{sads}.

Assuming the Langmuir model of adsorption for competitive chemisorption, the coverages of the IPA_{sads} and Ac_{sads} species on their common sites, at the adsorption equilibrium, in the presence of their partial pressures can be estimated according to

$$\theta_I = \frac{K_I P_I}{1 + K_I P_I + K_A P_A} \text{ and } \theta_A = \frac{K_A P_A}{1 + K_I P_I + K_A P_A} \quad (4)$$

where $K_I = K_I(0) \exp(E_I/RT)$ and $K_A = K_A(0) \exp(E_A/RT)$ are the adsorption coefficients for IPA and acetone (E_I and E_A are the heats of adsorption equal to the activation energies of desorption assuming nonactivated chemisorption). Using a numerical method, eq 4 provide θ_I and θ_A for coadsorption equilibrium according to the partial pressures P_I and P_A using simplified $K_I(0)$ and $K_A(0)$ expressions from the activated complex theory.[35] Considering the linear dependence of the heats of adsorption on θ_I and θ_A, eq 4 can be solved numerically. Theses calculations show that it is the IPA_{sads} species that cover the common s_1 sites even for the extreme situation with $P_A \gg P_I$; for instance, for $P_A = 395$ Pa and $P_I = 13$ Pa then $\theta_I = 0.955$ and $\theta_A = 0.045$.

Experimental Study of Competitive Chemisorption between IPA and Acetone. After the formation of Ac_{sads} at 300 K on TiO_2, Ac_g is removed and $P_I = 395$ Pa is introduced in the IR cell. It is observed (result not shown) the very fast (≈ 2 min) decrease in the coverage of Ac_{sads} (using the IR band at 1696 cm^{-1}) from $\theta_A = 1$ to $\theta_A = 0.23$ followed by a more progressive decrease to a constant value: $\theta_A = 0.1$, after 20 min of IPA adsorption. The comparison of these values with the coverage of Ac_{sads} after 40 min of desorption in a vacuum at 323 K (Figure 4), $\theta_A = 0.63$, shows clearly the impact of the competitive chemisorption. The steady-state coverage, $\theta_A = 0.1$, indicates that either IPA_{sads} cannot displace totally Ac_{sads} or more probably that a small fraction of the adsorption sites of the TiO_2 surface are specific of acetone (no competitive chemisorption). This has been confirmed performing the following experiment: after the formation of the IPA_{sads}, $P_A = 131$ Pa of acetone is introduced. The rapid appearance of the IR band at 1696 cm^{-1} is observed, indicating a coverage of $\theta_A = 0.08$, without any significant decrease in the IR bands of the IPA_{sads} species. These observations are consistent with the study of Bickley et al.,[8] who indicates that a small amount of acetone can be strongly adsorbed at 273 K (not removed by vacuum) on a TiO_2 surface covered by IPA_{sads}. This indicates that a small fraction of the TiO_2 sites is specific of the acetone adsorption (these sites are denoted s_2). Finally, the competitive chemisorption between IPA and acetone concerns roughly $404 \times 0.92 = 372$ μmol of s_1 sites/g, the remaining amount (32 μmol/g) corresponds to the s_2 sites. This has the following consequence: a large fraction of the s_1 sites is specific of the IPA_{sads} species. An acetone molecule formed by the PCO of a IPA_{sads} species adsorbed on those s_1 sites cannot remain adsorbed on the TiO_2 surface: it must either desorb rapidly as gaseous acetone or diffuse on the surface to be adsorbed on the s_2 sites (or on the s_1 sites liberated by the removal of IPA_{sads} species during the static O_2−PCO). Finally, during the PCO of IPA, if the coverage of the IPA_{sads} species is very high, the Ac_{sads} species can be only present on the s_2 sites. This is an important comment because it can be understood that the rate of formation of gaseous acetone is the highest and that of CO_2 is the lowest for high θ_I values (the coverage of the Ac_{ads} is very low). This competitive chemisorption between IPA and acetone leads to a new view of the elementary step S7: the activation energy of this elementary step must be considered significantly lower than that of Ac_{sads} on a clean TiO_2 surface ($E_{dAc}(1) = 87$ to $E_{dac}(0) = 108$ kJ/mol) excepted on the s_2 sites. However, during the O_2−PCO of IPA_{sads} (absence of gaseous IPA), the coverage θ_I progressively decreases and the gaseous acetone formed during the first minutes of the irradiation can be re-adsorbed on the fraction of

s_1 sites liberated by the conversion of IPA. This allows performing the deep oxidation of IPA_{sads}. In part 2, it is shown that a diffusion step of the Ac_{ads} species from the s1 sites to the s2 sites must be also involved in model M1.

During the deep O_2−PCO of IPA, water is produced according to reaction 1. Bickley et al.[8] suggest that competitive chemisorptions between H_2O/IPA and H_2O/acetone lead to the displacement of the organic molecules. These competitive chemisorptions have been studied at 300 K according to the following procedure: $P_{H_2O} = 395$ Pa has been introduced on a TiO_2 surface containing either IPA_{sads} or Ac_{sads} species. It has been observed (result not shown) that the intensities of the IR bands of the IPA_{sads} and Ac_{sads} species remain unchanged indicating the absence of a strong competitive chemisorption with H_2O. This is consistent with the results of Larson et al.,[9] who indicate that the introduction of a large amount of water on a TiO_2 surface saturated of acetone only displaces 21% of adsorbed acetone confirming that the competition H_2O/acetone is modest as compared to IPA/acetone (present study). The slight difference between the two studies is probably linked to the facts that (a) Larson et al.[9] use TiO_2 P25 (mixture anatase/rutile) that presents a difference of reactivity with (pure anatase)[41] and (b) the decrease by 21% probably corresponds to the displacement of weakly adsorbed species. Other literature data confirm that the competition chemisorption between IPA and H_2O is in favor of IPA: (a) Bickley et al.[8] indicates that preadsorption of H_2O on TiO_2 as a limited impact on the amount of IPA adsorbed and (b) Larson et al.[9] observe that gaseous H_2O is produced in parallel to gaseous acetone.

4. Conclusion

The present experimental microkinetic approach of the O_2−PCO of IPA on a TiO_2 catalyst of large BET area (335 m^2/g) according to the plausible kinetic model M1 leads to the following data on the surface elementary steps of interest:

(a) Step S1: The adsorption of IPA leads to the formation of two strongly adsorbed IPA species (undissociated and dissociated) and a weakly non dissociated IPA species (denoted IPA_{sads} and IPA_{wads}). The amount of IPA_{sads} is 940 μmol/g formed on TiO_2 sites denoted s1.

(b) Step S2: The activation energy of desorption of the IPA_{sads} species increases linearly with the decrease in the coverage from 118 to >178 kJ/mol at high and low coverages, respectively.

(c) Step S6: The IPA_{sads} species are oxidized in the absence ($O_{lat.}$−PCO) and in the presence of O_2 (O_2−PCO) into acetone, that is the single route to the deep O_2−PCO of IPA_g.

(d) Step S7: The adsorption of acetone on a clean TiO_2 surface leads to the formation of a single strongly adsorbed species: Ac_{sads} in a amount (404 μmol/g) significantly lower than IPA_{sads} species. A large fraction of the Ac_{sads} species is formed on the s_1 sites. The activation energy of desorption of the Ac_{sads} is lower than that of the IPA_{sads} species decreasing with the coverage from 87 kJ/mol to 108 μmol/g at high and low coverages.

(e) The activation energies of desorption of IPA_{sads} and Ac_{sads} indicate clearly that there is a strong competitive chemisorption in favor of IPA on the common s1 sites: IPA displaces adsorbed acetone species leading to a very small amount of acetone on the surface. However, a small amount of TiO_2 sites, 32 μmol/g, are specific of the acetone adsorption (there is no competitive chemisorption with IPA). The competitive chemisorption between the reactant IPA and the product acetone is a key process of the O_2−PCO of IPA because at high coverage of the surface by IPA, mainly gaseous acetone can be formed preventing the deep oxidation on IPA into CO_2.

In part 2 of the present study, it is shown that the various kinetic parameters determined in the present study associated to additional kinetic data (rate constant) of steps S6 and S8 allow us to provide a modeling of macroscopic kinetic data such as the evolutions, in Figure 6B, of (a) the coverage of IPA_{sads} and Ac_{sads} and (b) the acetone pressure as well as the TOF of the O_2−PCO of IPA using IPA/O_2 gas mixtures.

Acknowledgment. D.B acknowledges with pleasure FAURECIA, Systèmes d'échappements, Bois sur prés, 25 550, Bavans, France, for its financial support for the development of the experimental microkinetic approach of catalytic processes.

Nomenclature

EMA = experimental microkinetic approach

O_2−PCO and O_{lat}−PCO = photocatalytic oxidation in the presence and in the absence of O_2

IPA_{sads} and Ac_{sads} = strongly adsorbed IPA (two species: nondissociative, nd-, and dissociative, d-IPA_{sads}) and acetone species

X^*_{ads} = active oxygen containing adsorbed intermediate species of the O_2−PCO

$QIPA_{sads}$ and QAc_{sads} = amount of adsorbed IPA_{sads} and Ac_{sads} species on the TiO_2 surface

s1 = superficial sites of TiO_2 ($Ti^{+\delta}$ with different environments): 940 μmol/g, adsorbing IPA (there is a competitive chemisorption with acetone on a fraction α= (410/940) of the s_1 sites)

s2 = superficial $Ti^{+}\delta$ sites of TiO_2 sites: 32 μmol/g, specific of the acetone adsorption

θ_I, θ_A, θ_{X^*} = coverage of the TiO_2 surface by IPA_{sads} and Ac_{sads} (with and without competitive chemisorption) and of the X^*_{ads} species

$E_{dI}(\theta_I)$ and k_{dI} and $E_{dAc}(\theta_A)$ and k_{dAc} = activation energy and rate constant of desorption of IPA_{sads} and Ac_{sads} as a function of the coverage

K_I and P_I and K_A and P_A = adsorption coefficient and partial pressure of IPA and acetone

TOF = turnover frequency for the O_2−PCO of IPA

References and Notes

(1) Bourane, A.; Bianchi, D. *J. Catal.* **2003**, *220*, 3
(2) Bourane, A.; Bianchi, D. *J. Catal.* **2004**, *222*, 499.
(3) Retailleau, L.; Vonarb, R.; Perrichon, V.; Jean, E.; Bianchi. D. *Energy Fuels* **2004**, *18*, 872.
(4) Vonarb, R.; Hachimi, A.; Jean, E.; Bianchi, D. *Energy Fuels* **2005**, *19*, 35.
(5) Bianchi, D.; Emmanuel. J.; Ristori, A.; Vonarb, R. *Energy Fuels* **2005**, *19*, 1453.
(6) Dumesic, J. A.; et al. *The Microkinetics of Heterogeneous Catalysis*; ACS Professional Reference Book; American Chemical Society: Washington, DC, 1993.
(7) Boudart, M. *Catal. Lett.* **2000**, *65*, 1.
(8) Bickley, R. I.; Munuera, G.; Stone, F. S. *J. Catal.* **1973**, *31*, 398
(9) Larson, S. A.; Widegren, J. A.; Falconer, J. L. *J. Catal.* **1995**, *157*, 611.
(10) Brinkley, D.; Engel, T. *Surf. Sci.* **1998**, *415*, L1001.
(11) Brinkley, D.; Engel, T. *J. Phys. Chem. B* **1998**, *102*, 7596.
(12) Brinkley, D.; Engel, T. *J. Phys. Chem. B* **2000**, *104*, 9836.
(13) Formenti, M.; Juillet, F.; Meriaudeau, P.; Teichner, S. J. In *Proceeding of the 5th International Congress on catalysis 1972*; Hightower, J. W., Ed.; North-Holland, Amsterdam, 1973; p 1101.
(14) Herrmann, J. M.; Disdier, J.; Mozzanega, M. N.; Pichat, P. *J. Catal.* **1979**, *60*, 369.
(15) Xu, W.; Raftery, D.; Francisco. J. S. *J. Phys. Chem. B* **2003**, *107*, 4537.
(16) Ohko, Y.; Hashimoto, K.; Fujishima, A. *J. Phys. Chem. A* **1997**, *101*, 8057.

(17) Ohko, Y.; Hashimoto, K.; Fujishima, A. *J. Phys. Chem. B* **1998**, *102*, 1729.
(18) Muggli, D. S.; Falconer, J. L. *J. Catal.* **1999**, *187*, 230.
(19) Lee, G. D.; Falconer, J. L. *Catal. Lett.* **2000**, *70*, 145.
(20) Muggli, D. S.; Falconer, J. L. *J. Catal.* **2000**, *191*, 318.
(21) Bianchi D.; Gass, J. L. *J. Catal.* **1990**, *123*, 298.
(22) Herrmann, J. M. *Appl. Catal., A* **1997**, 156, 285.
(23) Wu, X.; Selloni, A.; Nayak, S. *J. Chem. Phys.* **2004**, *120*, 4512.
(24) Rasmussen, M. D.; Molina, L. M.; Hammer, B. *J. Chem. Phys* **2004**, *120*, 988.
(25) Czanderna A. W.; Honig, J. M. *J. Phys. Chem.* **1959**, *63*, 620.
(26) Bianchi, D.; Teichner, S. *J. Bull. Soc. Chim. Fr.* **1975**, *7*, 1463.
(27) Bourane, A.; Bianchi, D. *J. Catal.* **2002**, *209*, 114.
(28) El-Maazawi, M.; Finken, A. N.; Nair, A. B.; Grassian, V. H. *J. Catal.* **2000**, *191*, 138.
(29) Rossi, P. F.; Busca, G.; Lorenzelli, V.; Saur, O.; Lavalley, J. C. *Langmuir* **1987**, *3*, 52.
(30) Kim, K. S.; Barteau, M. A.; Farneth, W. E. *Langmuir* **1988**, *4*, 533.
(31) Rekoske, J. E.; Barteau, M. A. *J. Catal.* **1997**, *165*, 57.
(32) Gorte, R. J. *J. Catal.* **1982**, *75*, 75.
(33) Demmin, R. A.; Gorte, R. J. *J. Catal.* **1984**, *90*, 32.
(34) Derrouiche, S.; Bianchi, D. *Langmuir* **2004**, *124*, 116.
(35) Glasstone, S.; Laidler, K. J.; Eyring, H. *The Theory of Rate Processes*; McGraw-Hill: New York, 1941.
(36) Derrouiche, S.; Bianchi, D. *J. Catal.* **2005**, *230*, 359.
(37) Li, M.; Hebenstreit, W.; Diebold, U.; Tyryshkin, A. M.; Bowman, M. K.; Dunham, G. H.; Henderson, M. A. *J. Phys. Chem. B* **2000**, *104*, 4944.
(38) Henderson, M. A.; Epling, W. S.; Peden, C. H. F.; Perkins, C. L. *J Phys. Chem. B* **2003**, *107*, 534.
(39) Panov, A.; Fripiat, J. J. *Langmuir* **1998**, *14*, 3788.
(40) Zaki, M. I.; Hasan, M. A.; Pasupulety, L. *Langmuir* **2001**, *17*, 768.
(41) Luo, S.; Falconer, J. L. *J. Catal.* **1999**, *185*, 393.
(42) Bianchi, D.; Chafik, T.; Khalfallah, M.; Teichner, S. J. *Appl. Catal., A* **1993**, *105*, 223.